

1 Reventilation episodes during the sapropel S1 deposition in the eastern Mediterranean based on  
2 holococcolith preservation

3  
4 Alessandro Incarbona<sup>\*1</sup>, Ramadan H. Abu-Zied<sup>2</sup>, Eelco J. Rohling<sup>3,4</sup>, Patrizia Ziveri<sup>5,6</sup>

5  
6 <sup>1</sup>Università degli Studi di Palermo, Dipartimento di Scienze della Terra e del Mare, Via Archirafi  
7 20-22, 90134 Palermo, Italy

8 <sup>2</sup>Marine Chemistry Department, Faculty of Marine Sciences, King Abdulaziz University, P.O. Box  
9 80207, Jeddah 21589, Saudi Arabia

10 <sup>3</sup>Research School of Earth Sciences, The Australian National University, Canberra, ACT 2601,  
11 Australia

12 <sup>4</sup>Ocean and Earth Science, University of Southampton, National Oceanography Centre,  
13 Southampton, SO14 3ZH, United Kingdom

14 <sup>5</sup>Institute of Environmental Science and Technology (ICTA), Autonomous University of Barcelona  
15 (UAB), Bellaterra 08193, Spain

16 <sup>6</sup>Catalan Institution for Research and Advanced Studies (ICREA), Pg. Lluís Companys 23,  
17 Barcelona 08010, Spain

18  
19 \*Corresponding author: Alessandro Incarbona, e-mail: alessandro.incarbona@unipa.it; Telephone:  
20 +3909123864648

21  
22 Abstract

23 Organic-rich layers (sapropels) represent the most pronounced perturbations to thermohaline  
24 circulation and environmental conditions in the eastern Mediterranean, in response to enhanced  
25 African monsoon activity and subsequent massive freshwater discharge into the basin. During the  
26 most recent event, sapropel S1 formed between 10.8 and 6.1 ka, when freshwater-driven  
27 stratification caused seafloor anoxia below ~ 1800 metres depth, as a result of both failure of deep  
28 water formation and enhanced productivity. Here we analyse coccolith assemblages from the open  
29 eastern Mediterranean that form a West-East transect across the basin. We focus on holococcoliths,  
30 which are specifically produced by coccolithophores as part of their life cycle during their haploid  
31 phase. Since holococcolith calcification is characterised by nano-crystals highly susceptible to  
32 dissolution we are testing their potential preservation under different bottom environmental  
33 conditions, including the effect of post-depositional oxidation. The comparison with benthic  
34 foraminifera in a core recovered close to Lybia reveals that holococcolith preservation is enhanced  
35 during seafloor reventilation and benthic foraminiferal repopulation in the middle to upper part of  
36 the record, before the actual sapropel termination. There are two such events of improved deep  
37 water oxygenation in the Aegean and Adriatic Seas at 8.2 and 7.4 ka. The latter episode marks the  
38 onset of the transition to restored circulation in the eastern Mediterranean Sea, due to resumption of  
39 deep water formation in the southern Aegean Sea and the conclusion of enhanced biogenic  
40 productivity.

41  
42 Keywords

43 Coccoliths; preservation; DCM; *Florisphaera profunda*; Holocene.

44  
45 1 – Introduction

46 Organic-rich layers, the so-called sapropels, have repeatedly been deposited on the eastern  
47 Mediterranean sea-floor during precession minima [Hilgen, 1991]. Enhanced summer insolation  
48 strengthened African monsoon precipitation and led to massive freshwater discharge, especially via  
49 the Nile River during S1, but during other sapropels also including large fluxes from currently dry  
50 river systems along the wider North African margin [Rossignol-Strick et al., 1982; Rohling et al.,  
51 2002, 2004; Osborne et al., 2008]. Deep water formation was prevented by freshwater buoyancy

52 gain and a distinctive deep chlorophyll maximum (DCM) developed in the lower photic zone  
53 [*Rohling and Gieskes, 1989; Castradori, 1993; Kemp et al., 1999; Meier et al., 2004; De Lange et*  
54 *al., 2008; Rohling et al., 2015*].  
55 Sapropel S1 is the most recent organic-rich layer and is especially pronounced below 1800 m depth  
56 in the open eastern Mediterranean, between 10.8 and 6.1 kiloyears ago (ka) [*De Lange et al., 2008;*  
57 *Grant et al., 2016*]. Sapropel deposition was interrupted between 8.5 and 7.8 ka in the Aegean and  
58 Adriatic Seas [*Casford et al., 2003; Rohling et al., 2015*]. Intermittent bottom water ventilation is  
59 evident from the occurrence of benthic foraminifera faunas within S1 in the Aegean and Adriatic  
60 Seas and on the edge of the basin, offshore Libya and Israel [*Jorissen et al., 1993; Casford et al.,*  
61 *2003; Kuhnt et al., 2007; Abu-Zied et al., 2008; Schmiedl et al., 2010; Tesi et al., 2017*]. The short  
62 time scales of benthic foraminiferal repopulation events suggest the absence of an extensively  
63 anoxic water column. Anoxia may instead have ‘draped’ the seafloor like a thin ‘blanket’, whose  
64 occurrence would be governed by the balance between advective oxygen supply and biological and  
65 chemical oxygen consumption [*Casford et al., 2003*].  
66 Here we examine coccolith assemblages in S1 from three cores along a West-East transect across  
67 the eastern Mediterranean Sea. These cores were previously investigated and elemental proxies  
68 provide a precise estimate of the original vertical extent of sapropel S1 layers, including in the  
69 Libya offshore site where benthic foraminifera persistently survived [*Casford et al., 2003; Meier et*  
70 *al., 2004; Möbius et al., 2010*]. This study aims to assess paleoenvironmental changes across the  
71 eastern Mediterranean transect during sapropel S1 deposition. We pay special attention to coccolith  
72 preservation and selective dissolution of holococcoliths, because coccoliths produced during the  
73 holococcolithophore life stage seem to be especially prone to dissolution during early diagenesis  
74 [*Thomson et al., 2004; Crudeli et al., 2006; Incarbona and Di Stefano, 2018*]. Different processes  
75 occurred during S1 deposition may have altered the calcite saturation state, which at present is at  
76 supersaturated levels throughout the Mediterranean Sea [*Schneider et al., 2007*]: 1) increased  
77 primary productivity and water column oxygen shortage affect the extent and the strength of  
78 dissolution and thus the lysocline [*Paulmier et al., 2011; Barker, 2016*]; 2) the anoxic  
79 remineralization of  $C_{org}$  by sulphate reduction establishes an alkaline environment in interstitial pore  
80 waters, below the water/sediment interface [*Ten Haven et al., 1987; Thomson et al., 2004*]; 3)  
81 gypsum precipitation from Ca released by dissolving biogenic carbonate and  $SO_4$  released from  
82 pyrite oxydation [*Cita et al., 1977; Calvert, 1983; Ten Haven et al., 1987*] occurs upon post-  
83 depositional diffusion of oxygen into the sediment [*Van Santvoort et al., 1996; Thomson et al.,*  
84 *1999; De Lange et al., 2008*]. Our study of the three cores in the West-East transect is ideal for  
85 assessing potential holococcolith sensitivity to different water column and bottom environmental  
86 conditions, to test the effect of post-depositional oxidation and to estimate the existence of vertical  
87 (depth) offsets determined by aggressive pore water dissolution.

## 88 89 2 – Local setting

90 The Mediterranean Sea oceanographic circulation flows through three vertical layers in an overall  
91 anti-estuarine pattern. Surface waters from the Atlantic Ocean occupy the first 100-200 m depth  
92 (Modified Atlantic Water – MAW) and undergo severe evaporative salt-enrichment while they flow  
93 eastward [*POEM group, 1992; Millot, 1999*]. The northern branch of MAW in the Sicily Channel  
94 (Atlantic-Ionian Stream) enters the eastern Mediterranean Sea and feeds the Mid-Mediterranean Jet  
95 (MMJ) [*Robinson et al., 1999*] (Fig. 1). MAW describes a large cyclonic gyre into the eastern  
96 Mediterranean basin [*Pinardi and Masetti, 2000*]. The MMJ flows to the central Levantine Sea and  
97 then it turns northwards becoming the Cilician Current and the Asian Minor Current [*POEM group,*  
98 *1992; Pinardi and Masetti, 2000; Malanotte-Rizzoli et al., 2014*]. Our cores 562 and 569 are located  
99 within or very close to mesoscale anticyclonic gyres, core 563 is close to the MMJ path (Fig. 1).  
100 Levantine Intermediate Water (LIW) forms in winter due to surface cooling and evaporation near  
101 Rhodes [*Malanotte-Rizzoli and Hecht, 1988*]. LIW flows throughout the Mediterranean basin  
102 between 200 and 600 m depth and is a basic requisite for deep water formation. Eastern

103 Mediterranean Deep Water (EMDW) forms in the Adriatic and Aegean Sea and fills the Ionian and  
104 Levantine Sea bottom (Fig. 1) [POEM group, 1992]. Deep water formation in the Adriatic and  
105 Aegean Seas is promoted by winter heat flux loss, when northerlies blow [Josey et al., 2011;  
106 Rohling et al., 2015].

107 The eastern Mediterranean Sea is severely oligotrophic. Primary productivity reflects the nutrient  
108 depletion [Krom et al., 1991, 2010] and is relatively enhanced in winter, and very low in summer  
109 due to deepening of the thermocline and nutricline [Klein and Coste, 1984; Allen et al., 2002;  
110 D'Ortenzio and D'Alcalà, 2009]. Satellite analysis defines 562, 563 and 569 core sites as 'No  
111 Bloom' areas, with chlorophyll maxima centred between December and March [D'Ortenzio and  
112 D'Alcalà, 2009].

113

### 114 3 – Material and Methods

115 Multicores 562 (Gulf of Sirte, 32.774°N, 19.191°E, 1391 m water depth), 563 (South of Crete,  
116 33.718°N, 23.499°E, 1881 m water depth) and 569 (Eratosthenes seamount, 33.452°N, 32.576°E,  
117 1294 m water depth) were recovered during R/V Meteor cruise M51-3 (Fig. 1). A short  
118 sedimentological description is available in Meier et al. [2004] for 562 and 569. Both cores are  
119 made of nannofossil ooze with minor amounts of quartz and clay. The mismatch between Ba/Al and  
120 total organic carbon,  $\delta^{15}\text{N}$  and amino acid curves clearly testifies to the occurrence of a post-  
121 depositional oxygenation front marked by the Mn/Al peak, but there is no conclusive evidence for  
122 an S1 base, because the core did not reach that deep [Meier et al., 2004; Möbius et al., 2010] (Fig.  
123 2). No lithological description is available for core 563, but even in this case a clear post-  
124 depositional oxygenation front is visible from elemental proxies [Möbius et al., 2010] (Fig. 2).

125 Coccolith analysis was carried out at 1 cm resolution, between 29 and 4 cm below sea floor (cmbsf)  
126 for core 562, between 30 and 5 cmbsf for core 563 and between 31 and 9 cmbsf for core 569. The  
127 coccolith analysis was carried out by observation with a polarized microscope at 1000 X  
128 magnification. Rippled smear slides were prepared following the standard procedure [Bown and  
129 Young, 1998]. A mean of 500 specimens within the entire assemblage was identified following the  
130 taxonomic concepts for living coccolithophores of Young et al. [2003] and Jordan et al. [2004].  
131 Taxa were grouped in 'placoliths', 'miscellaneous group', 'upper photic zone (UPZ) group', 'lower  
132 photic zone (LPZ) group' and 'holococcoliths' [Di Stefano and Incarbona, 2004; Incarbona et al.,  
133 2010]. Placoliths include *Emiliania huxleyi*, small placoliths, small *Gephyrocapsa*, *Gephyrocapsa*  
134 *muelleriae* and *Gephyrocapsa oceanica*. Miscellaneous group includes *Helicosphaera* spp.,  
135 *Syracosphaera histrica*, *Pontosphaera* spp., *Calcidiscus leptoporus*, *Coronosphaera* spp.,  
136 *Braarudosphaera* spp., *Oolithotus fragilis*, *Calciosolenia* spp. and specimens of all the other  
137 species. UPZ group includes *Syracosphaera pulchra*, *Umbellosphaera* spp., *Discosphaera tubifera*,  
138 *Rhabdosphaera* spp. and *Umbilicosphaera* spp.. LPZ group includes *F. profunda* and a few  
139 specimens of *Gladiolithus flabellatus*. Holococcoliths include all the coccoliths produced during the  
140 holococcolithophore life stage.

141 Placoliths are r-strategist taxa: they grow and reproduce rapidly and bloom after nutrient  
142 fertilization [Young, 1994; Flores et al., 2000; Incarbona et al., 2010]. Among them, *E. huxleyi* is  
143 an opportunistic taxon that dominates today's ocean assemblages [Young, 1994]. In the  
144 Mediterranean Sea, this taxon blooms in winter and spring, after vertical convection that fuels  
145 nutrients into the photic zone [Knappertsbusch, 1993; Di Stefano et al., 2011]. LPZ taxa and the  
146 species *F. profunda* peak in response to nutricline deepening within the photic zone [Molfino and  
147 McIntyre, 1990b, 1990a; McIntyre and Molfino, 1996; Beaufort et al., 1997]. UPZ and  
148 Miscellaneous taxa are K-strategists (low division rate) to weakly K-strategists [Young, 1994;  
149 Incarbona et al., 2010]. Holococcoliths are produced by coccolithophores during their haploid life  
150 phase. Although belonging to different species, they behave as a homogeneous group [Oviedo et al.,  
151 2015], preferring warm and oligotrophic surface waters [Kleijne, 1991; Knappertsbusch, 1993;  
152 Oviedo et al., 2015; D'Amario et al., 2017].

153

#### 154 4 – Results

155 *Emiliania huxleyi* and *F. profunda* are the dominant taxa (Fig. 3-4). *Emiliania huxleyi* ranges  
156 between 37 and 68 % in core 562, 41 and 65 % in core 563, 33 and 64 % in core 569 and is  
157 respectively 51, 52 and 48 % on average. *Florisphaera profunda* ranges between 10 and 53 % in  
158 core 562, 13 and 53 % in core 563, 11 and 56 % in core 569 and is respectively 30, 29 and 33 % on  
159 average. Holococcoliths range between 1 and 16 % (6 % on average) in core 562, 1 and 14 % (7 %  
160 on average) in core 563 and 0 and 16 % (5 % on average) in core 569 (Fig. 4). Most of  
161 holococcolith specimens belong to *S. pulchra* HOL *oblonga* (*Calyptrorpha oblonga*), as already  
162 observed in late Quaternary Mediterranean sediments [Crudeli et al., 2006; Di Stefano et al., 2015;  
163 Incarbona and Di Stefano, 2018]. All the other taxa are largely subordinate and account for less  
164 than 5% (Fig. 3). These taxa provide useful paleoecological information once grouped following  
165 their ecological preference (Fig. 4). Placoliths and LPZ curves are identical to those from the  
166 dominant *E. huxleyi* and *F. profunda* species and their correlation index is  $R^2 = 0.70$ ,  $R^2 = 0.85$  and  
167  $R^2 = 0.94$  respectively for core 562, 563 and 569. UPZ and Miscellaneous taxa show opposite trends  
168 between the eastern and western sites and a few abundance variations that overcome the error for a  
169 95 % confidence level (Fig. 4).

170

#### 171 5 – Discussion

##### 172 5.1 – DCM and sapropel productivity

173 In all three 562, 563 and 569 cores, there is an evident *F. profunda* abundance increase within the  
174 sapropel S1 layer (Fig. 5), which points to a deep nutricline and a distinctive DCM. DCM  
175 development has been reported in all micropaleontological groups [Rohling and Gieskes, 1989;  
176 Castradori, 1993; Kemp et al., 1999; Meier et al., 2004] and is thought to be the reason for  
177 increased productivity and increased biogenic barite accumulation in sapropels [Rohling and  
178 Gieskes, 1989; Rohling et al., 2015]. This agrees with similarity between the *F. profunda* and Ba/Al  
179 profiles from the three cores (Fig. 5;  $R^2 = 0.65$  in core 562,  $R^2 = 0.63$  in core 563 and  $R^2 = 0.82$  in  
180 core 569). The dinoflagellate species *Leonella granifera*, a proxy for water stratification as a result  
181 of increased river input [Meier et al., 2004; Vink, 2004], shows the same pattern as *F. profunda* and  
182 Ba/Al in cores 562 and 569 [Meier et al., 2004].

183 *Florisphaera profunda* has been used as a proxy for paleoproductivity; more specifically, it was  
184 found to be inversely related to primary productivity in many low-latitude ocean settings [Beaufort  
185 et al., 1997; Hernández-Almeida et al., 2019]. This contrasts with enhanced productivity as inferred  
186 here for sapropel S1 by comparison with Ba/Al values. However, the behaviour of *F. profunda* in  
187 response to vertical column dynamics (stratification, upwelling and vertical convection) and in  
188 relation to productivity is not straightforward. There is a high correlation of organic carbon export  
189 and *F. profunda* fluxes in sediment traps of the Bay of Bengal and the Alboran Sea [Bárcena et al.,  
190 2004; Stoll et al., 2007]. Even more importantly, an extensive review of the *F. profunda* abundance  
191 and primary productivity relationship in all the oceans led to the conclusion that, with very few  
192 local exceptions, there is no inverse correlation in the Mediterranean Sea [Hernández-Almeida et  
193 al., 2019].

194 Looking at the spatial distribution of single signals, *F. profunda*, Ba/Al and *L. granifera* [Meier et  
195 al., 2004] seem to be quite different in the three sites. Among others, the Ba/Al is a perfect bell-  
196 shaped curve in core 569 and is asymmetric in 562 and 563 (Fig. 5). *Florisphaera profunda* shows a  
197 single abundance decrease in the lower-middle S1 in 562 and 563 cores and high-frequency  
198 variability in 569 (Fig. 5). This suggests that, although the DCM and high productivity are  
199 widespread features in the eastern Mediterranean Sea, local signals were superimposed, likely due  
200 to meso-scale oceanographic activity and surface and subsurface water dynamics. This local  
201 overprinting is supported by different trends in single species and groups, such as miscellaneous  
202 and UPZ taxa (Figs. 3-4).

203

##### 204 5.2 – Holococcolith preservation

205 There is a remarkable difference with the TOC pattern (as well as those of  $\delta^{15}\text{N}$  and the degradation  
206 index; Figure 2), which proves that there has been no influence of post-depositional sapropel  
207 oxidation ['burn down', *Van Santvoort et al.*, 1996; *Thomson et al.*, 1999; *De Lange et al.*, 2008] on  
208 holococcolith preservation (Fig. 5). In other words, holococcoliths were already dissolved or  
209 preserved once the oxygen penetrated the water/sediment interface at the end of sapropel  
210 deposition.

211 Benthic foraminiferal peaks within sapropel S1 of core 562 (Fig. 5) have contributed to formulation  
212 of the 'blanket' hypothesis; i.e. the occurrence of a thin anoxic layer on the seafloor occasionally  
213 displaced by intermittent dense water production and bottom ventilation in the Adriatic and Aegean  
214 Seas and in the basin edges [*Casford et al.*, 2003; *Kuhnt et al.*, 2007; *Abu-Zied et al.*, 2008;  
215 *Triantaphyllou et al.*, 2016]. The comparison between holococcolith and benthic foraminifera  
216 abundances reveals the presence of three different steps in the upper part of the record (Fig. 5). The  
217 oxyphilic benthic foraminifera peak at 17.5 cmbsf (Si in Fig. 5) correlates with the sapropel  
218 interruption in the Adriatic and Aegean Seas centred at about 8.2 ka [*Casford et al.*, 2003], likely  
219 due to monsoon activity weakening and/or northerly air outbreaks that led to surface cooling and  
220 temporary deep water formation [*Rohling et al.*, 1997, 2015, 2019; *Mercone et al.*, 2001; *Casford et*  
221 *al.*, 2003]. A small, but statistically significant (Fig. 4), peak in holococcoliths is found in the  
222 oxidised S1 in all cores and attests to improved preservation in coincidence with the reventilation  
223 episode at 8.2 ka (Fig. 5). Above 13.5 cmbsf, a peak in the absolute number of benthic foraminiferal  
224 specimens is again associated with improved holococcolith preservation. This horizon, which  
225 occurred well before the end of sapropel deposition, is especially relevant because also indicate the  
226 final decline of a distinct DCM combined with high primary productivity, as visible in *F. profunda*  
227 and Ba/Al patterns (Fig. 5). Thus, this level highlights the beginning of the transition from sapropel  
228 to modern environmental conditions in the eastern Mediterranean Sea, characterised by oligotrophic  
229 conditions with a short phytoplankton blooming (placolith-bearing species among  
230 coccolithophores) centred around winter/early spring [*Ziveri et al.*, 2000; *Auliahherliaty et al.*, 2009;  
231 *D'Ortenzio and D'Alcalà*, 2009; *Oviedo et al.*, 2015; *D'Amario et al.*, 2017]. The subsequent step at  
232 10.5 cmbsf, at the end of sapropel S1, led to persistent oxygen availability on the seafloor, re-  
233 population of oxyphilic benthic foraminifera assemblages and the preservation of holococcoliths  
234 that were resistant to pre-diagenetic dissolution [*Kleijne*, 1991]. The sequence described above is  
235 perfectly compatible with the occurrence of distinct reventilation episodes at 8.2 and 7.4 ka in the  
236 Aegean and Adriatic Seas, before the termination of sapropel deposition at 6.6-6.3 ka [*Filippidi et*  
237 *al.*, 2016]. Both the 8.2 and 7.4 ka events would be caused by cool and arid conditions that led to  
238 improved deep water oxygenation and benthic foraminiferal repopulation.

239 Though benthic foraminifera were not analysed in cores 563 and 569, we assume that enhanced  
240 holococcolith preservation is still able to provide evidence of seafloor oxygen availability. On this  
241 basis, the three steps are identified in the upper part of the holococcolith record in cores 563 and  
242 569 (Fig. 5). The only exception concerns an apparently missing holococcolith peak in core 569 at  
243 around the 8.2 ka event, which might be explained by the fact that this site is deeper than the 1800  
244 m depth limit below which persistent anoxia dominated throughout S1 [*De Lange et al.*, 2008].

245 Benthic foraminifera are usually present throughout the sapropel S1 layer in the Aegean Sea and the  
246 Adriatic Sea [*Jorissen et al.*, 1993; *Casford et al.*, 2003; *Kuhnt et al.*, 2007; *Abu-Zied et al.*, 2008;  
247 *Schmiedl et al.*, 2010], which indicates a continuous supply of (seasonal to interannual) oxygen  
248 from today's deep water formation sites that did not reach the open eastern Mediterranean Sea in  
249 sufficient volume. However, the three steps described above are still recognisable in the open  
250 eastern Mediterranean in terms of minor differences in benthic foraminifera assemblages,  
251 abundances, and derived oxygen indices on the eastern Mediterranean margin (Levantine Sea cores  
252 SL 112 and LC31) [*Schmiedl et al.*, 2010]. This suggests that the occurrence of a discrete number of  
253 oxygen availability phases across the open eastern Mediterranean Sea since the sapropel  
254 interruption, in sites that were above or close to the 1800 m depth limit of permanent anoxia.

255 Although detailed chronological constraints remain to be established for these events, the sequence

256 of improved deep water oxygenation in the Adriatic and Aegean Seas [Filippidi *et al.*, 2016] may  
257 provide a suitable explanation for this phenomenon.

258 Holococcoliths have a distinct preference for warm and oligotrophic water [Oviedo *et al.*, 2015] and  
259 may be able to adapt to ongoing Mediterranean climate change, where surface water would be  
260 characterised by relatively high calcite saturation state, high temperature, stratification and nutrient  
261 limitation [D'Amario *et al.*, 2017]. In accordance with their ecological preference, holococcoliths  
262 are especially abundant in eastern Mediterranean water samples [Oviedo *et al.*, 2015; D'Amario *et*  
263 *al.*, 2017]. Even though the Mediterranean waters are supersaturated with respect to calcite  
264 [Schneider *et al.*, 2007], holococcolith diversity and abundance are reduced in surface sediments  
265 [Kleijne, 1991; Knappertsbusch, 1993], because of disaggregation into microcrystals and  
266 lysocline/seafloor dissolution.

267 Poor holococcolith preservation within S1 may be explained by pre-diagenetic (lysocline)  
268 dissolution. The vertical lysocline extent and the calcite saturation state are affected by processes  
269 acting during sapropel deposition, including productivity variations and oxygen shortage [Paulmier  
270 *et al.*, 2011; Barker, 2016]. Since primary productivity was higher during S5 deposition than during  
271 S1 deposition, and since euxinia extended toward shallow levels near the base of the photic layer  
272 [Rohling *et al.*, 2006, 2015], different coccolith selective preservation might be expected in S5 than  
273 in S1. However, the coccolith distribution pattern during S5 is identical to S1, with no or rare  
274 holococcoliths and the preservation of delicate umbelliform species (i.e. *D. tubifera* and  
275 *Umbellosphaera* spp.) [Principato *et al.*, 2006], which suggests that lysocline dissolution was  
276 ineffective or negligible in explaining holococcolith absence in sapropel layers.

277 Late Quaternary sapropels are associated with high concentrations of aragonite, alternating with  
278 high-Mg calcite in underlying and overlying marls, both thought to be early diagenetic products  
279 [Calvert and Fontugne, 2001; Thomson *et al.*, 2004]. During S1 deposition, anoxic remineralization  
280 of C<sub>org</sub> by sulphate reduction would have enhanced sediment pore water alkalinity and thus  
281 enhanced diagenetic aragonite precipitation [Thomson *et al.*, 2004]. However, the only study  
282 dealing with interstitial sapropel waters indicates that the pH was significantly lower than in  
283 surrounding marls, due to anaerobic bacterial activity [Ten Haven *et al.*, 1987]. The role of bacterial  
284 activity in driving different seafloor preservation was identified through comparison of sediment  
285 trap and surface sediment coccolith assemblages in the Gulf of California [Ziveri and Thunell,  
286 2000]. There, a considerable number of species is lost (dissolved), and coccoliths show etching and  
287 fragmentation, on the anoxic seafloor due to organic acid production by bacteria and subsequent  
288 acidification of the water/sediment interface or of the top centimetres of the sediment column. In  
289 contrast, coccoliths are well preserved and the taxonomic composition of coccolithophores is much  
290 more similar to that observed in trap samples where bottom conditions are aerobic.

291 Scanning electron microscope (SEM) observation of coccoliths shows a prevalence of overgrowths  
292 in marls, and a prevalence of fragmentation/etching in S1 sediments [Crudeli and Young, 2003;  
293 Crudeli *et al.*, 2004]. This further supports that oxygen availability on the seafloor is key to  
294 holococcolith preservation in marls, and even within sapropel layers after episodes of reventilation.  
295 We also argue that holococcolith dissolution in S1 was limited to the top few centimetres of the  
296 sediment column, specifically < 9 cm in core 562, < 7 cm in core 563 and < 8 cm in core 569. These  
297 estimates relate to the thickness of the post-depositional sapropel 'burn down' (Fig. 2), which did  
298 not affect holococcolith preservation because they were already dissolved at the time of the initial  
299 oxygen penetration into the water/sediment interface.

300 The signal of *F. profunda* and Ba/Al decrease that marks the transition to modern eastern  
301 Mediterranean environmental conditions is widespread recorded, and is attributed to productivity  
302 decline in the photic zone, with limited to no impact of the seafloor oxygenation state. The abrupt  
303 decrease of *F. profunda* is seen throughout the Ionian, Adriatic, Aegean, and Levantine Seas  
304 [Giunta *et al.*, 2003; Principato *et al.*, 2003; Triantaphyllou *et al.*, 2009b, 2009a, 2010, 2016;  
305 Incarbona *et al.*, 2011; Incarbona and Di Stefano, 2018]. In cores 562, 563, and 569, this horizon  
306 resides 3-4 cm before the end of S1 deposition (Fig. 5). Assuming that the base of the sapropel is

307 very close to the base of sediment recovery at sites 562 and 563, and that S1 formed between 10.8  
308 and 6.1 ka [*Grant et al.*, 2016], we infer that the transition lasted about 750-1000 years. This  
309 duration estimate is much larger than a previous estimate of 100-200 years for re-oxygenation of the  
310 water column below 1500 m [*Casford et al.*, 2003]. However, the latter likely is an underestimate  
311 because it ignores the inventory of reduced chemical species in the water column that would need to  
312 be overcome, as well as the oxygen demand involved in re-oxidation ("burn down") of the sapropel  
313 after re-oxygenation of the overlying water column [*Casford et al.*, 2003]. Alternatively, the  
314 recovery of seafloor oxygenation may have suffered from a lower rate of dense water production,  
315 and consequently limited oxygen supply, relative to that involved in modern EMDW circulation. In  
316 any case, the 750-1000 years taken by the transition is compatible with the interval between  
317 restored deep water formation in the Aegean Sea (7.4 ka) and the end of sapropel deposition (6.3  
318 ka) [*Filippidi et al.*, 2016].

319

## 320 6 – Conclusions

321 Coccolith assemblages from three cores (M51-3 562, 563 and 569) along a West-East transect  
322 across the open eastern Mediterranean Sea have been investigated. Data from the most recent  
323 sapropel layer (S1) reveal development of a distinct DCM, indicated by increased abundance of *F.*  
324 *profunda*. A strong correlation between *F. profunda* and Ba/Al in all cores supports previous  
325 reconstructions that productivity especially increased in the lower photic zone [*Rohling and*  
326 *Gieskes*, 1989; *Castradori*, 1993; *Kemp et al.*, 1999; *Meier et al.*, 2004].

327 Comparison with TOC,  $\delta^{15}\text{N}$ , degradation index, Ba/Al and Mn/Al proves conclusively that there  
328 was no influence of post-depositional sapropel oxidation on holococcolith preservation. Sapropel S1  
329 holococcolith peaks in core 562 are associated with benthic foraminiferal repopulation episodes.  
330 The first episode can be correlated with sapropel interruption in the Adriatic and Aegean Seas. The  
331 second episode marks the onset of the transition to modern environmental conditions in the eastern  
332 Mediterranean Sea, coinciding with the final decline of high productivity. These two events are also  
333 visible in our other cores, except for the event associated with sapropel interruption in core 563,  
334 which is explained by the fact that this core was recovered from a site below the depth of permanent  
335 anoxia (De Lange et al., 2008). The two events are also compatible with reports of cool and arid  
336 conditions at 8.2 and 7.4 ka in the Aegean and Adriatic Seas [*Filippidi et al.*, 2016].

337

338 Acknowledgments: AI acknowledges funding by Italian Ministry of Education, Universities and  
339 Research through grant PJ\_RIC\_FFABR\_2017\_161560.

340

## 341 Bibliographic references

- 342 Abu-Zied, R. H., E. J. Rohling, F. J. Jorissen, C. Fontanier, J. S. L. Casford, and S. Cooke (2008),  
343 Benthic foraminiferal response to changes in bottom-water oxygenation and organic carbon  
344 flux in the eastern Mediterranean during LGM to Recent times, *Mar Micropaleontol*, 67(1–2),  
345 46–68, doi:10.1016/j.marmicro.2007.08.006.
- 346 Allen, J. I., P. J. Somerfield, and J. Siddorn (2002), Primary and bacterial production in the  
347 Mediterranean Sea: A modelling study, *J Mar Syst*, 33–34, 473–495, doi:10.1016/S0924-  
348 7963(02)00072-6.
- 349 Auliaherliaty, L., H. M. Stoll, P. Ziveri, E. Malinverno, M. V Triantaphyllou, S. Stravarakakis, and  
350 V. Lykousis (2009), Coccolith Sr/Ca ratios in the eastern Mediterranean: Production versus  
351 export processes, *Mar Micropaleontol*, 73(3–4), 196–206,  
352 doi:10.1016/j.marmicro.2009.10.001.
- 353 Bárcena, M. A., J. A. Flores, F. J. Sierro, M. Pérez-Folgado, J. Fabres, A. Calafat, and M. Canals  
354 (2004), Planktonic response to main oceanographic changes in the Alboran Sea (Western  
355 Mediterranean) as documented in sediment traps and surface sediments, *Mar Micropaleontol*,  
356 53(3–4), 423–445, doi:10.1016/j.marmicro.2004.09.009.
- 357 Barker, S. B. T.-R. M. in E. S. and E. S. (2016), Dissolution of Deep-Sea Carbonates, in

- 358 *PALEOCEANOGRAPHY, PHYSICAL AND CHEMICAL PROXIES*, edited by S. A. Elias,  
359 Elsevier.
- 360 Beaufort, L., Y. Lancelot, P. Camberlin, O. Cayre, E. Vincent, F. Bassinot, and L. Labeyrie (1997),  
361 Insolation Cycles as a Major Control of Equatorial Indian Ocean Primary Production, *Science*,  
362 278(5342), 1451–1454.
- 363 Bown, P. R., and J. R. Young (1998), Techniques, in *Calcareous Nannofossil Biostratigraphy*,  
364 edited by P. R. Bown, pp. 16–28, Chapman and Kluwer Academic, London.
- 365 Calvert, S. E. (1983), Geochemistry of Pleistocene sapropels from the eastern Mediterranean,  
366 *Oceanol Acta*, 6, 255–267.
- 367 Calvert, S. E., and M. R. Fontugne (2001), On the late Pleistocene-Holocene sapropel record of  
368 climatic and oceanographic variability in the eastern Mediterranean, *Paleoceanography*, 16(1),  
369 78–94, doi:10.1029/1999PA000488.
- 370 Casford, J. S. L., E. J. Rohling, R. H. Abu-Zied, C. Fontanier, F. J. Jorissen, M. J. Leng, G.  
371 Schmiedl, and J. Thomson (2003), A dynamic concept for eastern Mediterranean circulation  
372 and oxygenation during sapropel formation, *Palaeogeogr Palaeoclimatol Palaeoecol*, 190,  
373 103–119, doi:10.1016/S0031-0182(02)00601-6.
- 374 Castradori, D. (1993), Calcareous nannofossils and the origin of Eastern Mediterranean sapropel,  
375 *Paleoceanography*, 8(4), 459–471.
- 376 Cita, M. B., C. Vergnaud Grazzini, C. Robert, H. Chamley, N. Ciaranfi, and S. D’Onofrio (1977),  
377 Paleoclimatic record of long deep sea core from the eastern Mediterranean, *Quat Res*, 8, 205–  
378 235.
- 379 Crudeli, D., and J. R. Young (2003), SEM-LM STUDY OF HOLOCOCOLITHS PRESERVED  
380 IN EASTERN MEDITERRANEAN SEDIMENTS ( HOLOCENE / LATE PLEISTOCENE ),  
381 *J Nannoplankt Res*, 25(1), 39–50.
- 382 Crudeli, D., J. R. Young, E. Erba, G. J. De Lange, K. Henriksen, H. Kinkel, C. P. Slomp, and P.  
383 Ziveri (2004), Abnormal carbonate diagenesis in Holocene-late Pleistocene sapropel-  
384 associated sediments from the Eastern Mediterranean; Evidence from *Emiliania huxleyi*  
385 coccolith morphology, *Mar Micropaleontol*, 52(1–4), 217–240,  
386 doi:10.1016/j.marmicro.2004.04.010.
- 387 Crudeli, D., J. R. Young, E. Erba, M. Geisen, P. Ziveri, G. J. de Lange, and C. P. Slomp (2006),  
388 Fossil record of holococcoliths and selected hetero-holococcolith associations from the  
389 Mediterranean (Holocene-late Pleistocene): Evaluation of carbonate diagenesis and  
390 palaeoecological-palaeocenographic implications, *Palaeogeogr Palaeoclimatol Palaeoecol*,  
391 237(2–4), 191–212, doi:10.1016/j.palaeo.2005.11.022.
- 392 D’Amario, B., P. Ziveri, M. Grelaud, A. Oviedo, and M. Kralj (2017), Coccolithophore haploid and  
393 diploid distribution patterns in the Mediterranean Sea: Can a haplo-diploid life cycle be  
394 advantageous under climate change?, *J Plankton Res*, 39(5), 781–794,  
395 doi:10.1093/plankt/fbx044.
- 396 D’Ortenzio, F., and M. R. D’Alcalà (2009), On the trophic regimes of the Mediterranean Sea: A  
397 satellite analysis, *Biogeosciences*, 6(2), 139–148, doi:10.5194/bg-6-139-2009.
- 398 Filippidi, A., M. V. Triantaphyllou, and G. J. De Lange (2016), Eastern-Mediterranean ventilation  
399 variability during sapropel S1 formation, evaluated at two sites influenced by deep-water  
400 formation from Adriatic and Aegean Seas, *Quat Sci Rev*, 144, 95–106,  
401 doi:10.1016/j.quascirev.2016.05.024.
- 402 Flores, J. A., M. A. Bárcena, and F. J. Sierro (2000), Ocean-surface and wind dynamics in the  
403 Atlantic Ocean off Northwest Africa during the last 140 000 years, *Palaeogeogr*  
404 *Palaeoclimatol Palaeoecol*, 161(3–4), 459–478, doi:10.1016/S0031-0182(00)00099-7.
- 405 Giunta, S., a. Negri, C. Morigi, L. Capotondi, N. Combourieu-Nebout, K. C. Emeis, F. Sangiorgi,  
406 and L. Vigliotti (2003), Coccolithophorid ecostratigraphy and multi-proxy paleoceanographic  
407 reconstruction in the Southern Adriatic Sea during the last deglacial time (Core AD91-17),  
408 *Palaeogeogr Palaeoclimatol Palaeoecol*, 190, 39–59, doi:10.1016/S0031-0182(02)00598-9.



409 Grant, K. M., R. Grimm, U. Mikolajewicz, G. Marino, M. Ziegler, and E. J. Rohling (2016), The  
410 timing of Mediterranean sapropel deposition relative to insolation, sea-level and African  
411 monsoon changes, *Quat Sci Rev*, *140*, 125–141, doi:10.1016/j.quascirev.2016.03.026.

412 Ten Haven, H. L., G. J. De Lange, and R. E. McDuff (1987), Interstitial water studies of Late  
413 Quaternary Eastern Mediterranean sediments with emphasis on early diagenetic reactions and  
414 evaporitic salt influences, *Mar Geol*, *75*(1), 119–136, doi:https://doi.org/10.1016/0025-  
415 3227(87)90099-5.

416 Hernández-Almeida, I., B. Ausín, M. Saavedra-Pellitero, K.-H. Baumann, and H. M. Stoll (2019),  
417 Quantitative reconstruction of primary productivity in low latitudes during the last glacial  
418 maximum and the mid-to-late Holocene from a global *Florisphaera profunda* calibration  
419 dataset, *Quat Sci Rev*, *205*, 166–181, doi:https://doi.org/10.1016/j.quascirev.2018.12.016.

420 Hilgen, F. J. (1991), Astronomical calibration of Gauss to Matuyama sapropels in the  
421 Mediterranean and implication for the Geomagnetic Polarity Time Scale, *Earth Planet Sci Lett*,  
422 *104*(2–4), 226–244, doi:10.1016/0012-821x(91)90206-w.

423 Incarbona, A., and E. Di Stefano (2018), Calcareous nannofossil palaeoenvironmental  
424 reconstruction and preservation in sapropel S1 at the Eratosthenes Seamount (Eastern  
425 Mediterranean), *Deep Sea Res Part II Top Stud Oceanogr*, doi:10.1016/j.dsr2.2018.10.004.

426 Incarbona, A. et al. (2010), The Impact of the Little Ice Age on Coccolithophores in the Central  
427 Mediterranean Sea, *Clim Past*, *6*(6), 795–805, doi:10.5194/cp-6-795-2010.

428 Incarbona, A., P. Ziveri, N. Sabatino, D. S. Manta, and M. Sprovieri (2011), Conflicting  
429 coccolithophore and geochemical evidence for productivity levels in the Eastern  
430 Mediterranean sapropel S1, *Mar Micropaleontol*, *81*(3–4), 131–143,  
431 doi:10.1016/j.marmicro.2011.09.003.

432 Jordan, R. W., L. Cros, and J. R. Young (2004), A revised classification scheme for living  
433 haptophytes, edited by M. V Triantaphyllou, *Micropaleontology*, *50*, 55–79,  
434 doi:10.2113/50.Suppl\_1.55.

435 Jorissen, F. J., A. Asioli, A. M. Borsetti, L. Capotondi, J. P. de Visser, F. J. Hilgen, E. J. Rohling,  
436 K. van der Borg, C. Vergnaud Grazzini, and W. J. Zachariasse (1993), Late Quaternary central  
437 Mediterranean biochronology, *Mar Micropaleontol*, *21*(1–3), 169–189, doi:10.1016/0377-  
438 8398(93)90014-O.

439 Josey, S. A., S. Somot, and M. Tsimplis (2011), Impacts of atmospheric modes of variability on  
440 Mediterranean Sea surface heat exchange, *J Geophys Res Ocean*, *116*(2), 1–15,  
441 doi:10.1029/2010JC006685.

442 Kemp, A. E. S., R. B. Pearce, I. Koizumi, J. Pike, and S. J. Rance (1999), The role of mat-forming  
443 diatoms in the formation of Mediterranean sapropels, *Nature*, *398*, 57.

444 Kleijne, A. (1991), Holococcolithophorids from the Indian-Ocean, Red-Sea, Mediterranean-Sea and  
445 North-Atlantic Ocean, *Mar Micropaleontol*, *17*(1–2), 1–76, doi:Doi 10.1016/0377-  
446 8398(91)90023-Y.

447 Klein, P., and B. Coste (1984), Effects of wind-stress variability on nutrient transport into the mixed  
448 layer, *Deep Sea Res Part A Oceanogr Res Pap*, *31*(1), 21–37,  
449 doi:https://doi.org/10.1016/0198-0149(84)90070-0.

450 Knappertsbusch, M. (1993), Geographic distribution of living and Holocene coccolithophores in the  
451 Mediterranean Sea, *Mar Micropaleontol*, *21*(1–3), 219–247, doi:10.1016/0377-  
452 8398(93)90016-Q.

453 Krom, M. D., N. Kress, S. Brenner, and L. I. Gordon (1991), Phosphorus Limitation of Primary  
454 Productivity in the Eastern Mediterranean-Sea, *Limnol Oceanogr*, *36*(3), 424–432.

455 Krom, M. D., K. C. Emeis, and P. Van Cappellen (2010), Why is the Eastern Mediterranean  
456 phosphorus limited?, *Prog Oceanogr*, *85*(3–4), 236–244, doi:10.1016/j.pocean.2010.03.003.

457 Kuhnt, T., G. Schmiedl, W. Ehrmann, Y. Hamann, and C. Hemleben (2007), Deep-sea ecosystem  
458 variability of the Aegean Sea during the past 22 kyr as revealed by Benthic Foraminifera, *Mar  
459 Micropaleontol*, *64*(3), 141–162, doi:https://doi.org/10.1016/j.marmicro.2007.04.003.

- 460 De Lange, G. J., J. Thomson, A. Reitz, C. P. Slomp, M. S. Principato, E. Erba, and C. Corselli  
 461 (2008), Synchronous basin-wide formation and redox-controlled preservation of a  
 462 Mediterranean sapropel, *Nat Geosci*, *1*, 606–610, doi:10.1038/ngeo283.
- 463 Malanotte-Rizzoli, P., and A. Hecht (1988), Large-scale properties of the eastern Mediterranean: a  
 464 review., *Oceanol Acta*, *11*(4), 323–335, doi:10.1016/S0967-0645(99)00020-X.
- 465 Malanotte-Rizzoli, P. et al. (2014), Physical forcing and physical/biochemical variability of the  
 466 Mediterranean Sea: A review of unresolved issues and directions for future research, *Ocean*  
 467 *Sci*, *10*(3), 281–322, doi:10.5194/os-10-281-2014.
- 468 McIntyre, A., and B. Molino (1996), Forcing of Atlantic Equatorial and Subpolar Millennial  
 469 Cycles by Precession, *Science*, *274*(5294), 1867–1870, doi:10.1126/science.274.5294.1867.
- 470 Meier, K. J. S., K. A. F. Zonneveld, S. Kasten, and H. Willems (2004), Different nutrient sources  
 471 forcing increased productivity during eastern Mediterranean S1 sapropel formation as reflected  
 472 by calcareous dinoflagellate cysts, *Paleoceanography*, *19*(1), 1–12,  
 473 doi:10.1029/2003PA000895.
- 474 Mercone, D., J. Thomson, R. H. Abu-Zied, I. W. Croudace, and E. J. Rohling (2001), High-  
 475 resolution geochemical and micropalaeontological profiling of the most recent eastern  
 476 Mediterranean sapropel, *Mar Geol*, *177*(1–2), 25–44, doi:10.1016/S0025-3227(01)00122-0.
- 477 Millot, C. (1999), Circulation in the Western Mediterranean Sea, *J Mar Syst*, *20*(1–4), 423–442,  
 478 doi:10.1016/S0924-7963(98)00078-5.
- 479 Möbius, J., N. Lahajnar, and K. C. Emeis (2010), Diagenetic control of nitrogen isotope ratios in  
 480 Holocene sapropels and recent sediments from the Eastern Mediterranean Sea, *Biogeosciences*,  
 481 *7*(11), 3901–3914, doi:10.5194/bg-7-3901-2010.
- 482 Molino, B., and A. McIntyre (1990a), Nutricline variation in the equatorial Atlantic coincident  
 483 with the Younger Dryas, *Paleoceanography*, *5*(6), 997, doi:10.1029/PA005i006p00997.
- 484 Molino, B., and A. McIntyre (1990b), Precessional forcing of nutricline dynamics in the equatorial  
 485 Atlantic., *Science*, *249*(4970), 766–769, doi:10.1126/science.249.4970.766.
- 486 Osborne, A. H., D. Vance, E. J. Rohling, N. Barton, M. Rogerson, and N. Fello (2008), A humid  
 487 corridor across the Sahara for the migration of early modern humans out of Africa 120,000  
 488 years ago., *Proc Natl Acad Sci U S A*, *105*(43), 16444–16447, doi:10.1073/pnas.0804472105.
- 489 Oviedo, A., P. Ziveri, M. Álvarez, and T. Tanhua (2015), Is coccolithophore distribution in the  
 490 Mediterranean Sea related to seawater carbonate chemistry?, *Ocean Sci*, *11*, 13–32,  
 491 doi:10.5194/os-11-13-2015.
- 492 Paulmier, A., D. Ruiz-Pino, and V. Garçon (2011), CO<sub>2</sub> maximum in the oxygen minimum zone  
 493 (OMZ), *Biogeosciences*, *8*, 239–252, doi:10.5194/bg-8-239-2011.
- 494 Pinardi, N., and E. Masetti (2000), Variability of the large scale general circulation of the  
 495 Mediterranean Sea from observations and modelling: A review, *Palaeogeogr Palaeoclimatol*  
 496 *Palaeoecol*, *158*(3–4), 153–174, doi:10.1016/S0031-0182(00)00048-1.
- 497 POEM group (1992), General-Circulation of the Eastern Mediterranean, *Earth-Science Rev*, *32*(4),  
 498 285–309.
- 499 Principato, M. S., S. Giunta, C. Corselli, and A. Negri (2003), Late Pleistocene-Holocene  
 500 planktonic assemblages in three box-cores from the Mediterranean Ridge area (west-southwest  
 501 of Crete): Palaeoecological and palaeoceanographic reconstruction of sapropel S1 interval,  
 502 *Palaeogeogr Palaeoclimatol Palaeoecol*, *190*, 61–77, doi:10.1016/S0031-0182(02)00599-0.
- 503 Principato, M. S., D. Crudeli, P. Ziveri, C. P. Slomp, C. Corselli, E. Erba, and G. J. de Lange  
 504 (2006), Phyto- and zooplankton paleofluxes during the deposition of sapropel S1 (eastern  
 505 Mediterranean): Biogenic carbonate preservation and paleoecological implications,  
 506 *Palaeogeogr Palaeoclimatol Palaeoecol*, *235*(1–3), 8–27, doi:10.1016/j.palaeo.2005.09.021.
- 507 Robinson, A. R., J. Sellschopp, A. Warn-Varnas, W. G. Leslie, C. J. Lozano, P. J. Haley, L. a.  
 508 Anderson, and P. F. J. Lermusiaux (1999), The Atlantic Ionian stream, *J Mar Syst*, *20*(1–4),  
 509 129–156, doi:10.1016/S0924-7963(98)00079-7.
- 510 Rohling, E. J., and W. W. Gieskes (1989), Late Quaternary changes in Mediterranean intermediate

- 511 water density and formaton rate, *Paleoceanography*, 4(5), 531–545.
- 512 Rohling, E. J., F. J. Jorissen, and H. C. De stigter (1997), 200 Year interruption of Holocene  
513 sapropel formation in the Adriatic Sea, *J Micropalaeontology*, 16(2), 97–108,  
514 doi:10.1144/jm.16.2.97.
- 515 Rohling, E. J. et al. (2002), African monsoon variability during the previous interglacial maximum,  
516 *Earth Planet Sci Lett*, 202(1), 61–75, doi:https://doi.org/10.1016/S0012-821X(02)00775-6.
- 517 Rohling, E. J. et al. (2004), Reconstructing past planktic foraminiferal habitats using stable isotope  
518 data: A case history for Mediterranean sapropel S5, *Mar Micropaleontol*, 50(1–2), 89–123,  
519 doi:10.1016/S0377-8398(03)00068-9.
- 520 Rohling, E. J., E. C. Hopmans, and J. S. S. Damsté (2006), Water column dynamics during the last  
521 interglacial anoxic event in the Mediterranean (sapropel S5), *Paleoceanography*, 21(2), 1–8,  
522 doi:10.1029/2005PA001237.
- 523 Rohling, E. J., G. Marino, and K. M. Grant (2015), Mediterranean climate and oceanography, and  
524 the periodic development of anoxic events (sapropels), *Earth-Science Rev*, 143,  
525 doi:10.1016/j.earscirev.2015.01.008.
- 526 Rohling, E. J., G. Marino, K. M. Grant, P. A. Mayewski, and B. Weninger (2019), A model for  
527 archaeologically relevant Holocene climate impacts in the Aegean-Levantine region  
528 (easternmost Mediterranean), *Quat Sci Rev*, 208, 38–53,  
529 doi:https://doi.org/10.1016/j.quascirev.2019.02.009.
- 530 Rossignol-Strick, M., W. Nesteroff, P. Olive, and C. Vergnaud-Grazzini (1982), After the deluge:  
531 Mediterranean stagnation and sapropel formation, *Nature*, 295, 105.
- 532 Van Santvoort, P. J. M., G. J. De Lange, J. Thomson, H. Cussen, T. R. S. Wilson, M. D. Krom, and  
533 K. Ströhle (1996), Active post-depositional oxidation of the most recent sapropel (S1) in  
534 sediments of the eastern Mediterranean Sea, *Geochim Cosmochim Acta*, 60(21), 4007–4024,  
535 doi:10.1016/S0016-7037(96)00253-0.
- 536 Schmiedl, G., T. Kuhnt, W. Ehrmann, K.-C. Emeis, Y. Hamann, U. Kotthoff, P. Dulski, and J.  
537 Pross (2010), Climatic forcing of eastern Mediterranean deep-water formation and benthic  
538 ecosystems during the past 22 000 years, *Quat Sci Rev*, 29(23), 3006–3020,  
539 doi:https://doi.org/10.1016/j.quascirev.2010.07.002.
- 540 Schneider, A., D. W. R. Wallace, and A. Körtzinger (2007), Alkalinity of the Mediterranean Sea,  
541 *Geophys Res Lett*, 34(15), doi:10.1029/2006GL028842.
- 542 Di Stefano, A., L. M. Foresi, A. Incarbona, M. Sprovieri, M. Vallefucio, M. Iorio, N. Pelosi, E. Di  
543 Stefano, P. Sangiorgi, and F. Budillon (2015), Mediterranean coccolith ecobiostratigraphy  
544 since the penultimate Glacial (the last 145,000years) and ecobioevent traceability, *Mar*  
545 *Micropaleontol*, 115, doi:10.1016/j.marmicro.2014.12.002.
- 546 Di Stefano, E., and A. Incarbona (2004), High-resolution palaeoenvironmental reconstruction of  
547 ODP Hole 963D (Sicily Channel) during the last deglaciation based on calcareous  
548 nanofossils, *Mar Micropaleontol*, 52(1–4), doi:10.1016/j.marmicro.2004.04.009.
- 549 Di Stefano, E., A. Incarbona, S. Bonomo, and N. Pelosi (2011), Coccolithophores in water samples  
550 and fossil assemblages in sedimentary archives of the Mediterranean Sea: A review, in *New*  
551 *Oceanography Research Developments: Marine Chemistry, Ocean Floor Analyses and Marine*  
552 *Phytoplankton*, edited by L. Martorino and K. Puopolo, pp. 127–162, Nova Science Publishers,  
553 Inc.
- 554 Stoll, H. M., A. Arevalos, A. Burke, P. Ziveri, G. Mortyn, N. Shimizu, and D. Unger (2007),  
555 Seasonal cycles in biogenic production and export in Northern Bay of Bengal sediment traps,  
556 *Deep Res Part II Top Stud Oceanogr*, 54(5–7), 558–580, doi:10.1016/j.dsr2.2007.01.002.
- 557 Tesi, T., A. Asioli, D. Minisini, V. Maselli, G. Dalla Valle, F. Gamberi, L. Langone, A. Cattaneo, P.  
558 Montagna, and F. Trincardi (2017), Large-scale response of the Eastern Mediterranean  
559 thermohaline circulation to African monsoon intensification during sapropel S1 formation,  
560 *Quat Sci Rev*, 159, 139–154, doi:10.1016/j.quascirev.2017.01.020.
- 561 Thomson, J., D. Mercone, G. J. De Lange, and P. J. M. Van Santvoort (1999), Review of recent

562 advances in the interpretation of eastern Mediterranean sapropel S1 from geochemical  
563 evidence, *Mar Geol*, 153(1–4), 77–89, doi:10.1016/S0025-3227(98)00089-9.

564 Thomson, J., D. Crudeli, G. J. De Lange, C. P. Slomp, E. Erba, C. Corselli, and S. E. Calvert  
565 (2004), Florisphaera profunda and the origin and diagenesis of carbonate phases in eastern  
566 Mediterranean sapropel units, *Paleoceanography*, 19(3), 1–19, doi:10.1029/2003PA000976.

567 Triantaphyllou, M. V. et al. (2016), Holocene Climatic Optimum centennial-scale  
568 paleoceanography in the NE Aegean (Mediterranean Sea), *Geo-Marine Lett*, 36(1), 51–66,  
569 doi:10.1007/s00367-015-0426-2.

570 Triantaphyllou, M. V et al. (2009a), Late Glacial-Holocene climate variability at the south-eastern  
571 margin of the Aegean Sea, *Mar Geol*, 266(1–4), 182–197, doi:10.1016/j.margeo.2009.08.005.

572 Triantaphyllou, M. V et al. (2009b), Late Glacial-Holocene ecostratigraphy of the south-eastern  
573 Aegean Sea, based on plankton and pollen assemblages, *Geo-Marine Lett*, 29(4), 249–267,  
574 doi:10.1007/s00367-009-0139-5.

575 Triantaphyllou, M. V, A. Antonarakou, M. D. Dimiza, and C. Anagnostou (2010), Calcareous  
576 nannofossil and planktonic foraminiferal distributional patterns during deposition of sapropels  
577 S6, S5 and S1 in the Libyan Sea (Eastern Mediterranean), *Geo-Marine Lett*, 30(1), 1–13,  
578 doi:10.1007/s00367-009-0145-7.

579 Vink, A. (2004), Calcareous dinoflagellate cysts in South and equatorial Atlantic surface sediments:  
580 diversity, distribution, ecology and potential for palaeoenvironmental reconstruction, *Mar*  
581 *Micropaleontol*, 50(1), 43–88, doi:https://doi.org/10.1016/S0377-8398(03)00067-7.

582 Young, J. R. (1994), Functions of coccoliths, in *Coccolithophores*, edited by A. Winter and W. G.  
583 Siesser, pp. 63–82, Cambridge Univ. Press, Cambridge.

584 Young, J. R., M. Geisen, L. Cros, A. Kleijne, C. Sprengel, I. Probert, and J. Østergaard (2003), A  
585 guide to extant coccolithophore taxonomy, *J Nannoplankt Res*, (Special Issue 1), 125.

586 Ziveri, P., and R. C. Thunell (2000), Coccolithophore export production in Guaymas Basin, Gulf of  
587 California: response to climate forcing, *Deep Res Part II*, 47(9–11), 2073–2100,  
588 doi:http://dx.doi.org/10.1016/S0967-0645(00)00017-5.

589 Ziveri, P., A. Rutten, G. J. De Lange, J. Thomson, and C. Corselli (2000), Present-day coccolith  
590 fluxes recorded in central eastern Mediterranean sediment traps and surface sediments,  
591 *Palaeogeogr Palaeoclimatol Palaeoecol*, 158(3–4), 175–195, doi:10.1016/S0031-  
592 0182(00)00049-3.

#### 593 Captions

594 Figure 1: Bathymetric map of the eastern Mediterranean Sea and cores location. The black arrow  
595 indicates the path of MAW. The black circles indicate the location of M51-3 562, 563 and 569  
596 cores. AIS: Atlantic Ionian Stream. MMJ: Mid-Mediterranean Jet. CC-AMC: Cilician Current and  
597 Asian Minor Current. A: Adriatic Sea deep water formation site. B: Anticyclone in the Gulf  
598 of Sirte. C: Aegean Sea deep water formation site. D: Western Cretan Gyre and intermediate water  
599 formation site. E: Shikmona summer Gyre.

600  
601  
602 Figure 2: Downcore variations of geochemical and benthic foraminifera data at 562, 563 and 569  
603 cores plotted *versus* depth (centimetres below sea floor - cmbfsf). Black and dashed lines in Ba/Al  
604 and Mn/Al curves respectively refer to data from Möbius *et al.* [2010] and Meier *et al.* [2004]. The  
605 vertical dark grey band indicates the extent of visible sapropel S1. The vertical light grey band  
606 indicates the extent of burn down sapropel S1.

607  
608 Figure 3: Downcore variations of selected coccolith species at 562, 563 and 569 cores plotted  
609 *versus* depth (centimetres below sea floor - cmbfsf). Black lines are 3-pt running averages. Vertical  
610 bars show the 95 % confidence level error associated to the counting for each taxon. The vertical  
611 dark grey band indicates the extent of visible sapropel S1. The vertical light grey band indicates the  
612 extent of burn down sapropel S1.

613  
614  
615  
616  
617  
618  
619  
620  
621  
622  
623  
624  
625  
626  
627  
628

Figure 4: Downcore variations of coccolith groups at 562, 563 and 569 cores plotted *versus* depth (centimetres below sea floor - cmbsf). Black lines are 3-pt running averages. Vertical bars show the 95 % confidence level error associated to the counting for each taxon. The vertical dark grey band indicates the extent of visible sapropel S1. The vertical light grey band indicates the extent of burn down sapropel S1.

Figure 5: Downcore variations of coccolith taxa, geochemical and benthic foraminifera data at 562, 563 and 569 cores plotted *versus* depth (centimetres below sea floor - cmbsf). Black and red lines in the benthic foraminifera plot respectively indicate absolute numbers of specimens and oxyphilic taxa percentage values. Si marks the sapropel interruption in the Adriatic and Aegean Sea. Vertical dashed lines mark the transition to modern environmental conditions in the eastern Mediterranean Sea. The vertical dark grey band indicates the extent of visible sapropel S1. The vertical light grey band indicates the extent of burn down sapropel S1.

Figure 1.



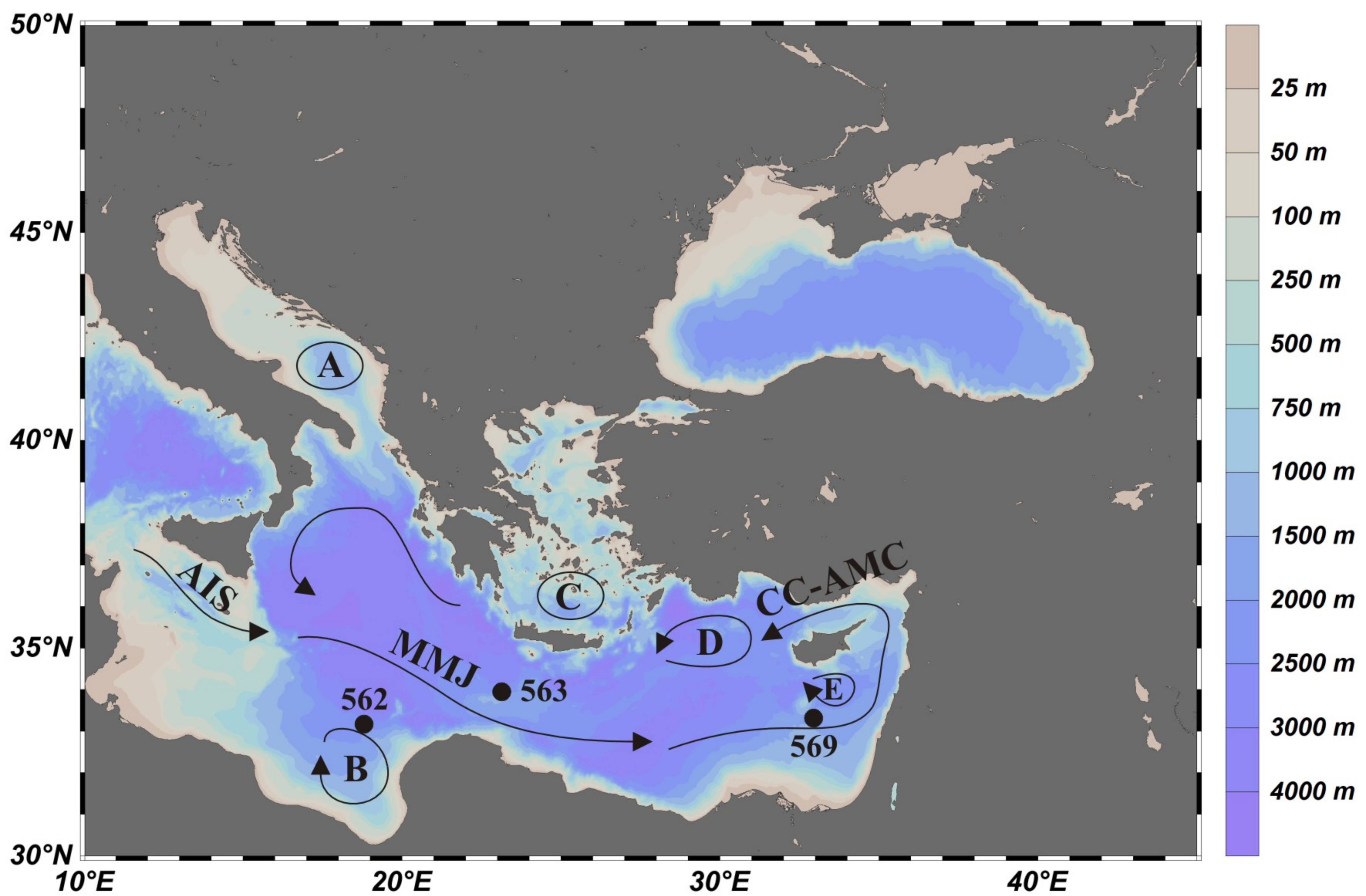


Figure 2.



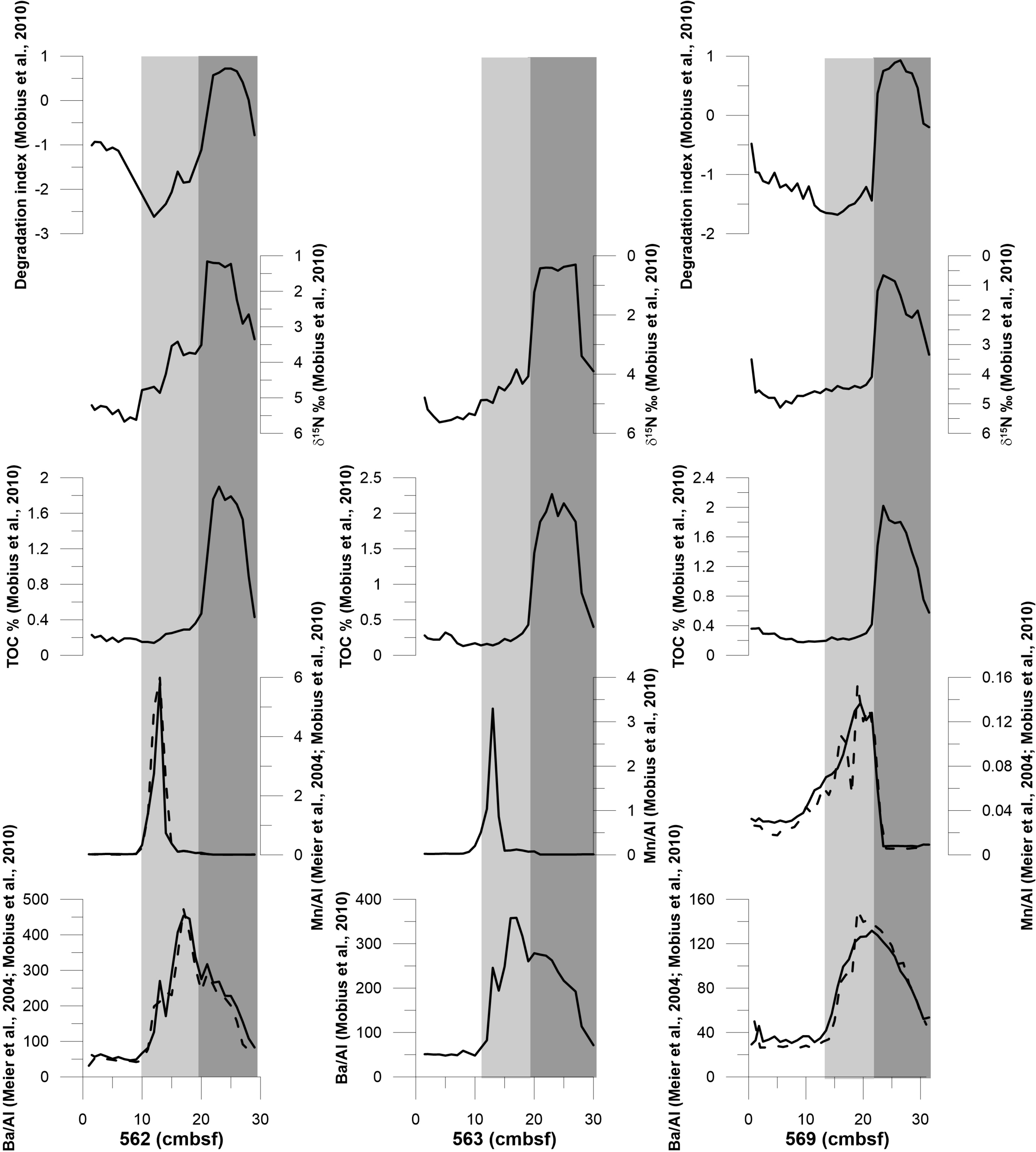
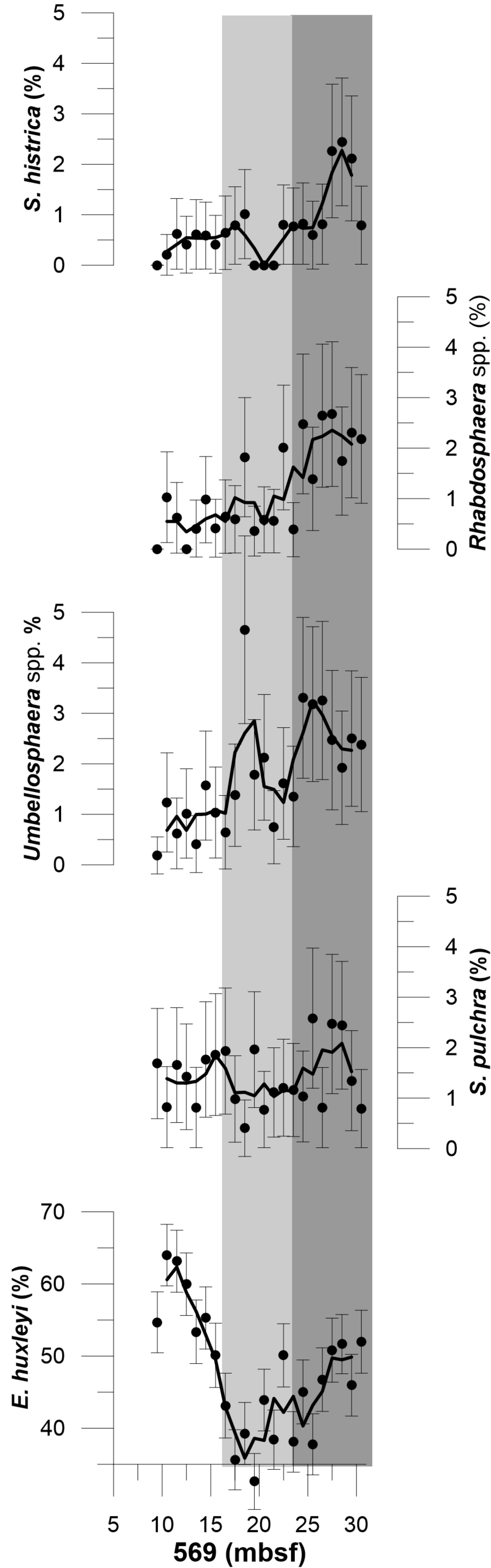
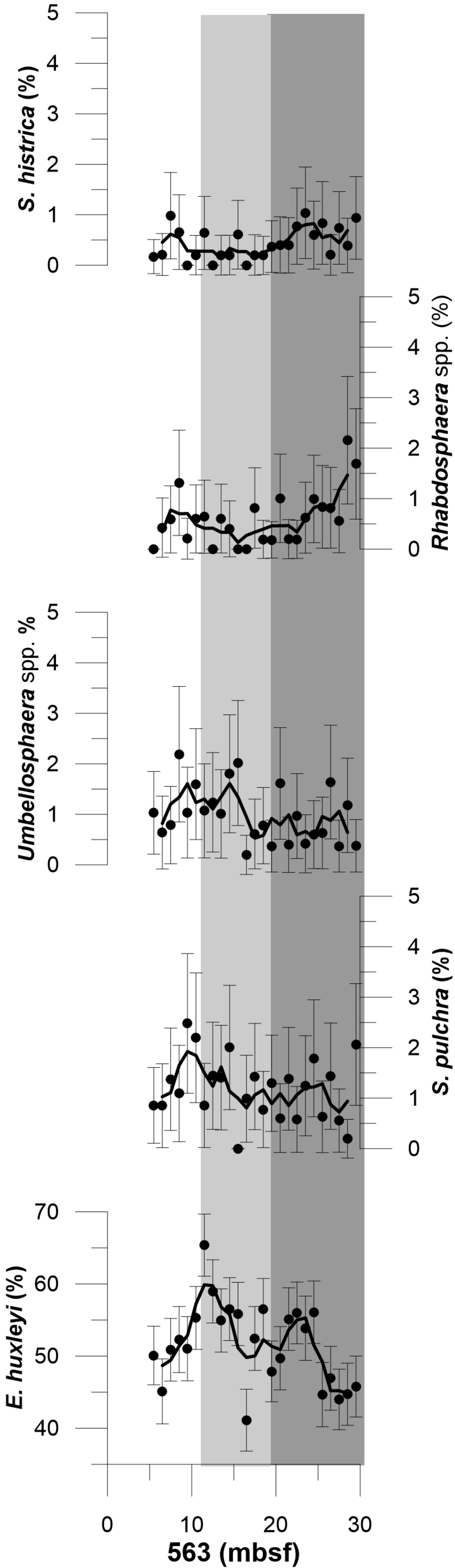
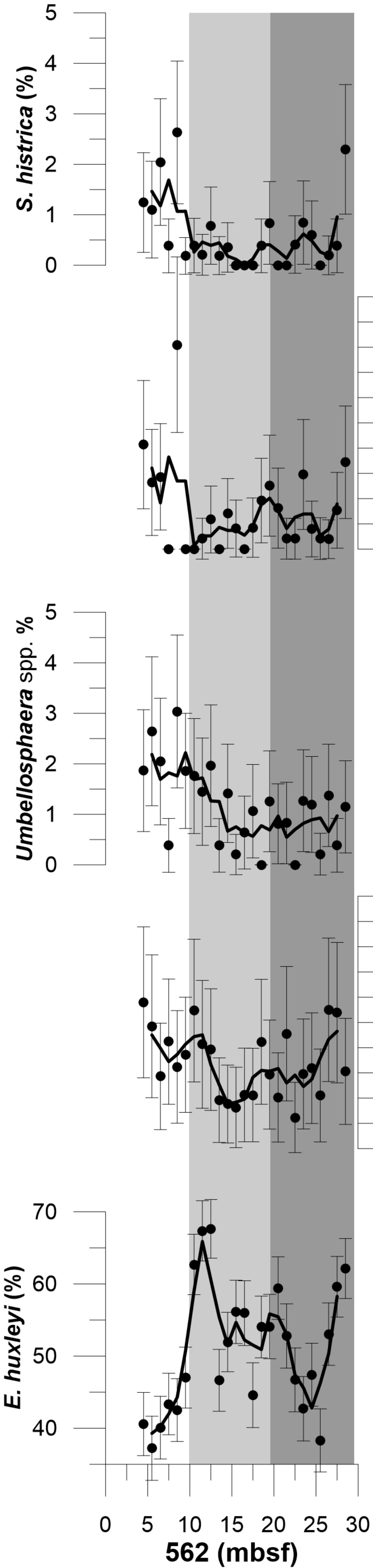


Figure 3.



**Figure 4.**



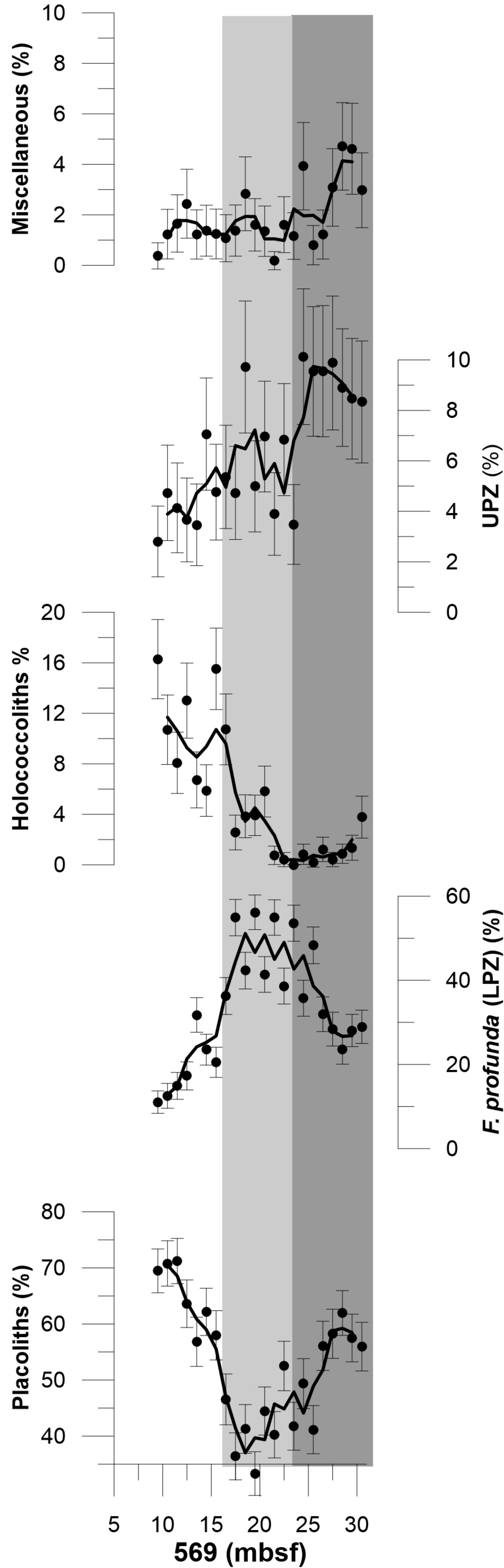
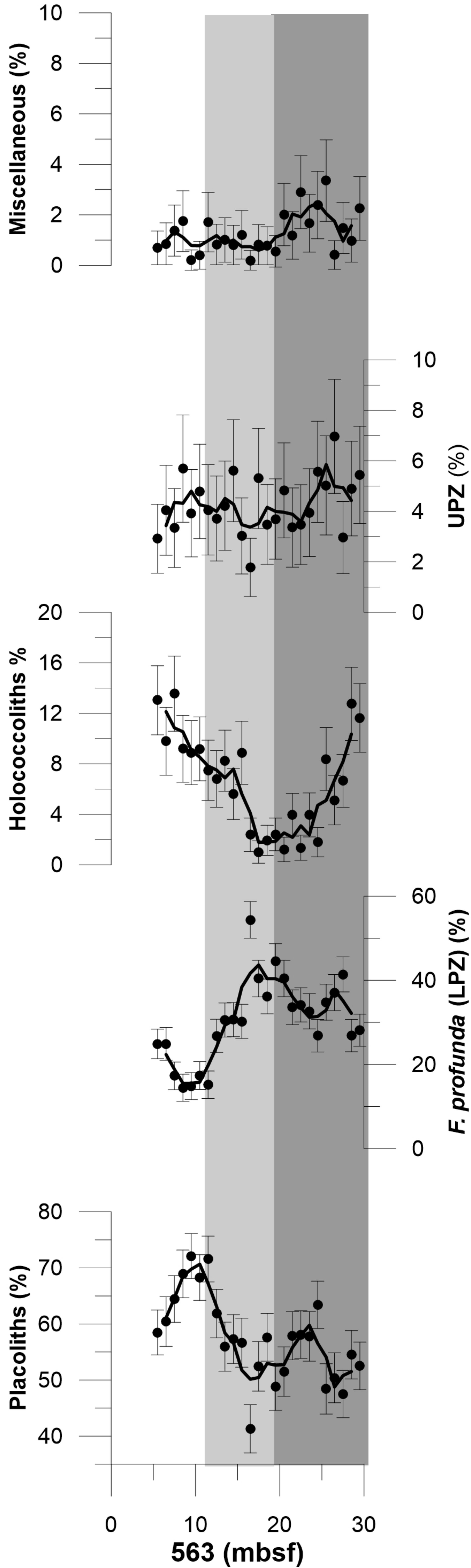
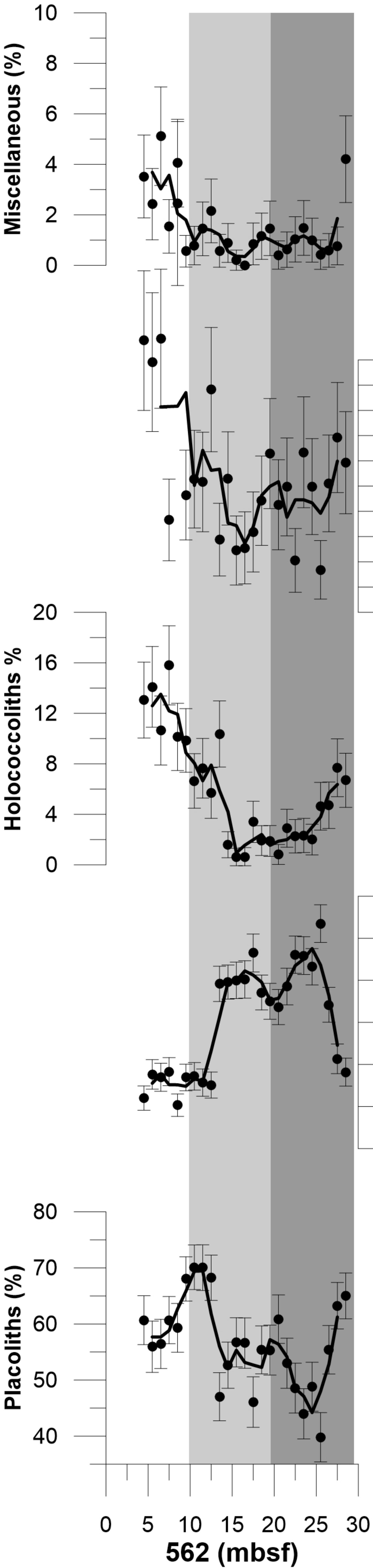


Figure 5.



